



Conformational changes induced by high-pressure homogenization inhibit myosin filament formation in low ionic strength solutions



Xing Chen ^a, Xinglian Xu ^{a,*}, Minyi Han ^a, Guanghong Zhou ^a, Conggui Chen ^b, Peijun Li ^b

^a Key Laboratory of Animal Products Processing, Ministry of Agriculture, Key Laboratory of Meat Processing and Quality Control, Ministry of Education, Jiangsu Synergetic Innovation Center of Meat Production and Processing, and College of Food Science and Technology, Nanjing Agricultural University, Nanjing, Jiangsu 210095, People's Republic of China

^b School of Biology and Food Engineering, Hefei University of Technology, Hefei, Anhui 230009, People's Republic of China

ARTICLE INFO

Article history:

Received 20 January 2016

Received in revised form 30 March 2016

Accepted 9 April 2016

Available online 16 April 2016

Keywords:

Myofibrillar proteins

Myosin

High-pressure homogenization

Conformation

Solubility

Filament formation

ABSTRACT

Myofibrillar proteins (MPs) of chicken breast are generally insoluble in water. We have developed a new method whereby MPs are solubilized in water by applying high-pressure homogenization (HPH) thus potentially enabling greater utilization of meat in various products. To clarify the mechanism of solubilization of MPs by HPH, we investigated their conformation, solubility and filament forming behavior in low ionic strength solutions induced by 15,000 psi HPH (103 MPa). HPH induces unfolding of MPs which subsequently exposes sulfhydryl and hydrophobic groups to the surface. Our findings, determined by circular dichroism, ATR-FTIR, SDS-PAGE and LC-ESI-MS/MS analysis suggest that HPH leads to unraveling of helical structures and to formation of myosin oligomers through disulfide bond. Due to intermolecular electrostatic repulsion and physical barrier of disulfide bonds in the rod induced by HPH, we suggest that the altered myosin conformation in MPs inhibits filament formation, thus contributing to high solubility of MPs in water.

© 2016 Elsevier Ltd. All rights reserved.

1. Introduction

Myofibrillar proteins (MPs), comprised of approximately 50% of the total meat proteins, are not readily soluble in low ionic strength solutions or water. The low solubility of MPs is largely attributed to the spontaneous formation of myosin (major protein in MPs) filaments that occurs *in vitro* at low ionic strength (Chen et al., 2016b). A relatively high concentration of salt (>0.3 M NaCl or KCl) is required for their complete solubilization (Ito, Tatsumi, Wakamatsu, Nishimura, & Hattori, 2003). To increase the utilization of meat, particularly from lower-value cuts, there is a need to determine if MPs can be solubilized at low ionic strength under certain conditions. For example, producing meat products in the form of liquid diet together with low salt for elderly people and dysphagic patients with malnutrition (Nieuwenhuizen, Weenen, Rigby, & Hetherington, 2010; Tokifuji, Matsushima, Hachisuka, & Yoshioka, 2013).

Many studies have investigated the solubilization of MPs in water or low ionic strength media and the mechanism has been determined (Chen et al., 2016b; Hayakawa, Ito, Wakamatsu, Nishimura, & Hattori, 2009; Ito et al., 2003; Katayama, Haga, & Saeki, 2004; Katayama & Saeki, 2007; Takai, Yoshizawa, Ejima, Arakawa, & Shiraki, 2013). More

than 80% of MPs from chicken breast were solubilized in a low ionic strength solution containing 5 mM histidine (His) by washing and ultrasonication of muscle tissues (Ito et al., 2003). It was suggested that 5 mM His might affect the secondary structure of myosin (Guo, Peng, Zhang, Liu, & Cui, 2015) and cause elongation of light meromyosin (LMM), resulting in the inhibition of native myosin filament formation (Hayakawa et al., 2009; Hayakawa, Ito, Wakamatsu, Nishimura, & Hattori, 2010). Ultrasonication was used for disruption of the highly-ordered structure of the myofibrils and their solubilization in a low ionic strength solution (1 mM KCl) (Ito et al., 2003). In a physiological salt solution (0.15 M), 50 mM arginine was found to increase the equilibrium solubility and activation energy of self-association of monomeric porcine myosin (Takai et al., 2013). Through the Maillard reaction, water-soluble MPs from fish or shellfish can be prepared by glycosylation with glucose (Katayama, Shima, & Saeki, 2002; Saeki & Inoue, 1997). The increase in negative charge repulsion among myosin molecules and the introduction of the glycosyl units onto the surface of the rod region provide repulsive electrostatic and steric forces which prevent the self-assembly of myosin molecules in low ionic strength medium, thus improving their solubility (Katayama et al., 2004). These results suggest that solubility of MPs depend on the conformational characteristics and the association state of myosin in low ionic strength solutions.

Recently, we established a new method to facilitate solubilization of chicken breast MPs in water without degradation of individual protein polypeptides by applying 15,000 psi (103 MPa) high-pressure

* Corresponding author.

E-mail addresses: cxniigata@163.com (X. Chen), xlxus@njau.edu.cn (X. Xu), redleafnew@163.com (M. Han), ghzhou@njau.edu.cn (G. Zhou), chen_conggui@hotmail.com (C. Chen), li_pj@hotmail.com (P. Li).

homogenization (HPH) treatment (Chen, Xu, & Zhou, 2016a). Furthermore, we demonstrated that HPH induced a reduction in particle size and a strengthening of intermolecular electrostatic repulsion of MPs in water. However, the reason that HPH improves the solubility and stability of MPs remains unclear. It has been reported that the cavitation phenomena, high shearing and turbulence by the strong force of HPH can affect the macromolecular conformation of soy and whey proteins (Keerati-u-rai & Corredig, 2009; Lee, Lefèvre, Subirade, & Paquin, 2007; Liu & Kuo, 2016). Therefore, the objective of the present study was to determine the behavior and conformation of MPs solubilized in water induced by treatment with HPH and to elucidate the solubilization mechanism by comparison with the native soluble MPs in high ionic strength solution (0.6 M NaCl, pH 7.0).

2. Materials and methods

2.1. Materials

The frozen chicken breast used during this research was purchased from a local market (Sushi Food Co., Ltd., Nanjing, China).

2.2. Preparation of water soluble MPs by HPH

The frozen chicken breast was thawed for about 12 h at 4 °C and washed chicken breast myofibrils were prepared as previously reported (Chen et al., 2016a). Briefly, the minced meat (100 g) was washed four times with cold (4 °C) deionized, distilled water. In each washing step the mince and water (1:10 w/v) were allowed to sit for 10 min after an initial homogenization (Ultraturrax T25, IKA, Staufen, Germany) at 8000 rpm for 2 min. The collected sediment after the final step of washing and centrifugation was termed washed myofibrils. Washed myofibrils were then suspended in water or 0.6 M NaCl solution (pH 7.0).

According to our procedure (Chen et al., 2016a), the myofibril dispersions were subjected to 15,000 psi (103 MPa) HPH treatment for two passes by using a high pressure homogenizer (Mini DeBee, Bee International, USA) equipped with a single pressure intensifier and a 75- μ m opening Y-type diamond nozzle (Genizer™, Los Angeles, USA) in a modular homogenization cell. The homogenized dispersions were centrifuged at 20,000 g for 20 min and the resulting supernatants were used as HPH induced water-soluble MPs (H-WSMP). For comparison, washed myofibrils suspended in 0.6 M NaCl (pH 7.0) were centrifuged at 20,000 g for 20 min and the resulting supernatants were used as salt-soluble MPs (SSMP). Washed myofibrils suspended in 0.6 M NaCl (pH 7.0) were also treated by HPH with the same procedure of H-WSMP and the resulting supernatants were prepared as HPH treated salt-soluble MPs (H-SSMP). Where preparations were subsequently dialysed with dialysis bags (diameter: 36 mm, MW: 3500 Da) against 1 mM NaCl solution (pH 7.0) they are identified as D-H-WSMP, D-SSMP and D-H-SSMP.

2.3. Protein electrophoresis of water soluble MPs

2.3.1. Reducing sodium dodecyl sulfate–polyacrylamide gel electrophoresis (reducing SDS-PAGE) and non-reducing SDS-PAGE

Reducing or non-reducing SDS-PAGE was run with a 4% acrylamide stacking gel and a 10% separating gel to observe the original myofibrillar constituents and the cross-linked protein polymers as previously described (Li, Xiong, & Chen, 2012). Protein samples (2 mg/mL) were mixed with an equal volume of sample buffer without or with 5% β -mercaptoethanol (β -ME) then boiled for 4 min. Each well was loaded with 10 μ L of samples or markers. The electrophoretic analysis was performed on a Bio-Rad Mini-PROTEAN II System Cell apparatus (Bio-Rad Laboratories Inc., Hercules, CA, USA) at a constant voltage of 120 V for 1 h. The stained gel was scanned by using Imager Scanner III (EU-88, Epson, Japan) and the densities of bands were analyzed by Quantity One software (Bio-Rad, Laboratories Inc., Benicia, CA, USA).

2.3.2. Nano liquid chromatography-electrospray ionization-mass spectrometry/mass spectrometry (Nano LC-ESI-MS/MS) analysis

For Nano LC-ESI-MS/MS analysis, protein bands in the gels were excised manually and digested with trypsin. The peptides from the digestion were extracted with acetonitrile, and then completely dried in a SpeedVac device (Thermo, CA, USA). The dried samples were then re-dissolved in sample solution (2% acetonitrile, 97.5% water, 0.5% formic acid). Each protein solution was reduced by DTT and all cysteine residues were alkylated by iodo-acetamide and cleaned. The samples were then digested with sequencing-grade modified trypsin (Promega, MI, USA) in digestion buffer (100 mM ammonium bicarbonate, pH 8.5). Following digestion, the peptides were analyzed using an ion trap mass spectrometer (LTQ Linear Ion Trap Mass Spectrometer System (Thermo, CA, USA) coupled with a high pressure liquid chromatography (HPLC) system. All MS data were searched in the non-redundant protein database (NR database, NCBI). The relative abundance of protein in a sample (excised protein band) was determined based on a label-free quantitation method (Griffin et al., 2010).

2.4. Conformational characteristics of water soluble MPs

2.4.1. Reactive sulfhydryl (SH) groups and surface hydrophobicity determination

Determination of reactive SH groups was carried out according to the method as previous described (Chen et al., 2014) with slight modifications. Fifty microliters of 10 mM DTNB solution (20 mM phosphate buffer, pH 8.0) was added to 4 mL of the sample (1 mg/mL) and the reaction was allowed to proceed for 20 min at 25 °C. The absorbance of the mixture was measured at 412 nm with a Microplate Reader (SpectraMax M2, Molecular Devices Limited, USA). The content of sulfhydryl groups was expressed as micromoles of SH per 100 mg protein, using a molar extinction coefficient ($EM = 13,600$).

The surface hydrophobicity was measured using 8-anilino-1-naphthalene sulphonic acid (ANS) as previously described (Cao, Xia, Zhou, & Xu, 2012) with slight modifications. Ten microlitres of 15 mM ANS solution (in 0.1 M phosphate buffer, pH 7.0) was added to 2 mL of the sample (1 mg/mL). After leaving for 20 min at 25 °C, the fluorescence was determined (SpectraMax M2, Molecular Devices Limited, USA) using an excitation wavelength of 380 nm and an emission wavelength in the range of 410 to 570 nm at a 300-nm/min scanning speed. The surface hydrophobicity was expressed as fluorescence intensity (arbitrary units, a.u.).

2.4.2. Secondary structure analysis by circular dichroism (CD) and Attenuated total reflectance-Fourier transform infrared (ATR-FTIR) spectroscopy

The CD spectrum was measured using a Jasco J-715 spectropolarimeter (Jasco Co. Ltd., Tokyo, Japan). The soluble MPs (0.3 mg/mL) were transferred to a quartz cell with a 0.1 cm light-path. Molecular ellipticity was measured in the range from 200 to 240 nm at a scan rate of 20 nm/min at a regulated temperature. The percentages of α -helix structures were determined using the protein secondary structure estimation program (Yang's method) provided with the Jasco J-715 spectro-polarimeter.

ATR-FTIR spectroscopy was performed on a Thermo-Fisher Nicolet 6700 spectrometer (Thermo Electric Corporation, IL, USA) using a DTGS (KBr beamsplitter) detector with Smart iTX accessory (Li & Xiong, 2015). Each spectrum from 400 to 4000 cm^{-1} was collected with an average of 256 scans at a resolution of 4 cm^{-1} . Buffer background samples to determine the effects of water or 0.6 M NaCl solutions were subtracted before collecting a sample spectra. Fourier self-deconvolution of merged FTIR scans from three independent MP samples (5 mg/mL) were obtained and a quantitative estimation of α -helix content was made on the assumption that any protein can be considered as the linear sum of a few fundamental secondary structural elements and the percentage of each element was only related to

the spectral intensity (Kong & Yu, 2007) by using Omnic software (Thermo Electric Corporation, IL, USA).

2.5. Solubility and filament formation in low ionic strength solution (1 mM NaCl, pH 7.0)

It is known that native myosin (major protein in MPs) assembles and forms a filamentous polymer under low ionic strength conditions *in vitro*, resulting in low solubility in low ionic strength solutions. For determination of the solubility and filament formation at low ionic strength, the H-WSMP, SSMP and H-SSMP were dialyzed against low ionic strength solution (1 mM KCl, pH 7.0) for 48 h according to a previous procedure (Hayakawa et al., 2009). The corresponding dialyzed samples were deemed as D-H-WSMP, D-SSMP and D-H-SSMP, respectively.

2.5.1. Solubility

The non-dialyzed or dialyzed samples were centrifuged at 20,000 g for 20 min. The solubility was expressed as percent of protein concentration in the supernatant with respect to that of protein in samples before centrifugation (Chen et al., 2016b). The protein concentrations were determined by the Biuret method.

2.5.2. Dynamic light scattering (DLS) measurement of particle size

DLS is a useful technology to monitor myosin filament dissociation or monomer aggregation by measuring the hydrodynamic radius of particles in the solution (Chen et al., 2016b; Shimada, Takai, Ejima, Arakawa, & Shiraki, 2015). DLS measurement was performed as previously reported (Shimada et al., 2015) with a slight modification by using a Zetasizer Nano ZS 90 (Malvern Instruments, Worcestershire, UK) equipped with a 4 mW He–Ne ion laser ($\lambda = 633$ nm). The protein samples (0.5 mg/mL) were placed in a 1-cm path-length quartz cuvette and subjected to DLS measurement with a detection angle of 90° at 25 ± 0.1 °C. Hydrodynamic diameters of myosin particles were estimated from the auto-correlation function, using the Cumulants method, based on a single exponential fit of the auto-correlation function to obtain the mean particle size (average hydrodynamic diameter).

2.6. Statistical analysis

All data are presented as mean \pm SD (standard deviation) values of three or four independent experiments. The analyses of variances, means and SDs were analyzed with the Statistical Analysis System (SAS Institute Inc., Cary, NC, USA). A $P < 0.05$ significance level was used to determine the differences between the treatments.

3. Results and discussion

3.1. Protein profiles of H-WSMP, SSMP and H-SSMP

Individual protein compositions of H-WSMP, SSMP and H-SSMP and their cross-linked patterns were visualized through non-reducing and reducing SDS-PAGE (Fig. 1). A typical polypeptide composition of MPs was observed in the SSMP samples both in the absence (Fig. 1C) or presence of β -ME (Fig. 1D); the major MP components corresponding to myosin heavy chain (MHC) and actin were consistent with a previous report (Hayakawa et al., 2009). However for H-WSMP, a water-soluble oligomer band was seen at the top of the separating gel in the non-reducing SDS-PAGE pattern (Fig. 1A), indicating a different protein profile to that of native MPs in 0.6 M NaCl (Fig. 1C). As compared to SSMP, there was a significant reduction in the amount of MHC from H-WSMP (Fig. 1A). When H-WSMP was treated with β -ME, the oligomer band completely vanished while the lost MHC was mostly recovered (Fig. 1B). It is likely that the water-soluble oligomers present in the H-WSMP were largely derived from myosin with disulfide bonds. To verify this, the corresponding bands including oligomer 1, MHC 2 and

MHC 3 (Fig. 1A and B) were excised for Nano LC-ESI-MS/MS analysis and protein identification. The results showed that all the protein bands contained relative high abundance of myosin heavy chain: 60.4%, 70.3% and 97.0% for oligomer 1, MHC 2 and MHC 3, respectively (Table 1), confirming the existence of soluble myosin oligomer in the H-WSMP. It has been demonstrated that HPH (65 MPa) causes changes in the supramolecular structure of soy proteins and formation of soluble aggregates with high average molecular mass (Keerati-u-rai & Corredig, 2009). Protein aggregations in MPs treated at 20,000 psi (138 MPa) HPH were also discovered in our previous study (Chen et al., 2016a). Thus, it was expected that the soluble myosin oligomer in H-WSMP might be induced by HPH. Since no such kind of myosin oligomer was detected in SSMP (Fig. 1C and D), our immediate interest was in testing whether HPH can indeed cause the formation of soluble myosin oligomer in SSMP. When SSMP was subjected to HPH treatment under the same conditions used for H-WSMP, there was a reduction in the amount of MHC which corresponded with the production of a similar oligomer band that remained on the top of the non-reducing pattern of H-SSMP (Fig. 1E). Reducing the sample with β -ME regained most of the MHC from the oligomer (Fig. 1F). Additionally, myosin heavy chain was also identified as the dominant species (Table 1) in the excised protein band (oligomer 4, MHC 5 and MHC 6 in Fig. 1E and F). Therefore, we concluded that HPH produced soluble myosin oligomers in H-WSMP and H-SSMP and it was likely that they were primarily cross linked via disulfide bonds.

The combined forces of high velocity impact, high-frequency vibration, instantaneous pressure drop, intense shear, cavitation and high pressures with a short treatment time (less than 5 s) induced by HPH can affect the macromolecular conformation of proteins (Liu & Kuo, 2016; Liu et al., 2010). As myosin is the predominant component of MPs, conformational changes in myosin of the H-WSMP and H-SSMP were expected. Cross-linking of myosin subjected to HPH treatment occurred in MPs, for which oxidation of the SH groups to form disulfide links played a major role. It is suggested that formation of free radicals during the HPH process could have occurred as was observed by Yuan, Gao, Zhao, and Mao (2008) and Pereda, Ferragut, Quevedo, Guamis, and Trujillo (2007) when β -carotene was degraded and lipid oxidation increased as a consequence of HPH (> 100 MPa) treatment. Under the modification of free radicals, which commonly occurs in muscle foods during manufacturing and storage, studies have demonstrated that oxidative conversion of SH groups of cysteine residues to S-S bonds in the rod portion is a principal reaction occurring in the dimerization and polymerization of myosin, which change the functionality of MPs (Li et al., 2012; Ooizumi & Xiong, 2006; Xiong, Park, & Ooizumi, 2008). Although 9 of the 16 cysteine residues in MHC are located in the myosin globular head (S1), it has been reported that their susceptibility to intramolecular S-S bond formation under oxidative conditions provides opportunity for other cysteine residues in the unraveled rod region to participate in inter-molecular cross-linking (Li & Xiong, 2015). Myosin oligomer-soluble filament complex via tail-tail cross-linking was also observed by TEM during heating (Shimada et al., 2015). These previous results led us to hypothesize that soluble myosin oligomers in MPs were induced through S-S bonding in the rod during HPH process, determining its protein functionality. Further information is needed to specify the location of disulfide cross-linking formed in myosin.

3.2. Reactive SH groups and surface hydrophobicity of H-WSMP, SSMP and H-SSMP

As the marker of protein unfolding, reactive SH groups and surface hydrophobicity of H-WSMP, SSMP and H-SSMP were determined (Fig. 2). Compared to SSMP, the reactive groups and surface hydrophobicity of H-WSMP and H-SSMP were both significantly increased, suggesting the exposure of SH groups to the proteins surface. Similar results of exposed and hydrophobic site changes have been observed in trypsin (Liu et al., 2010) and soy protein (Liu & Kuo, 2016) after

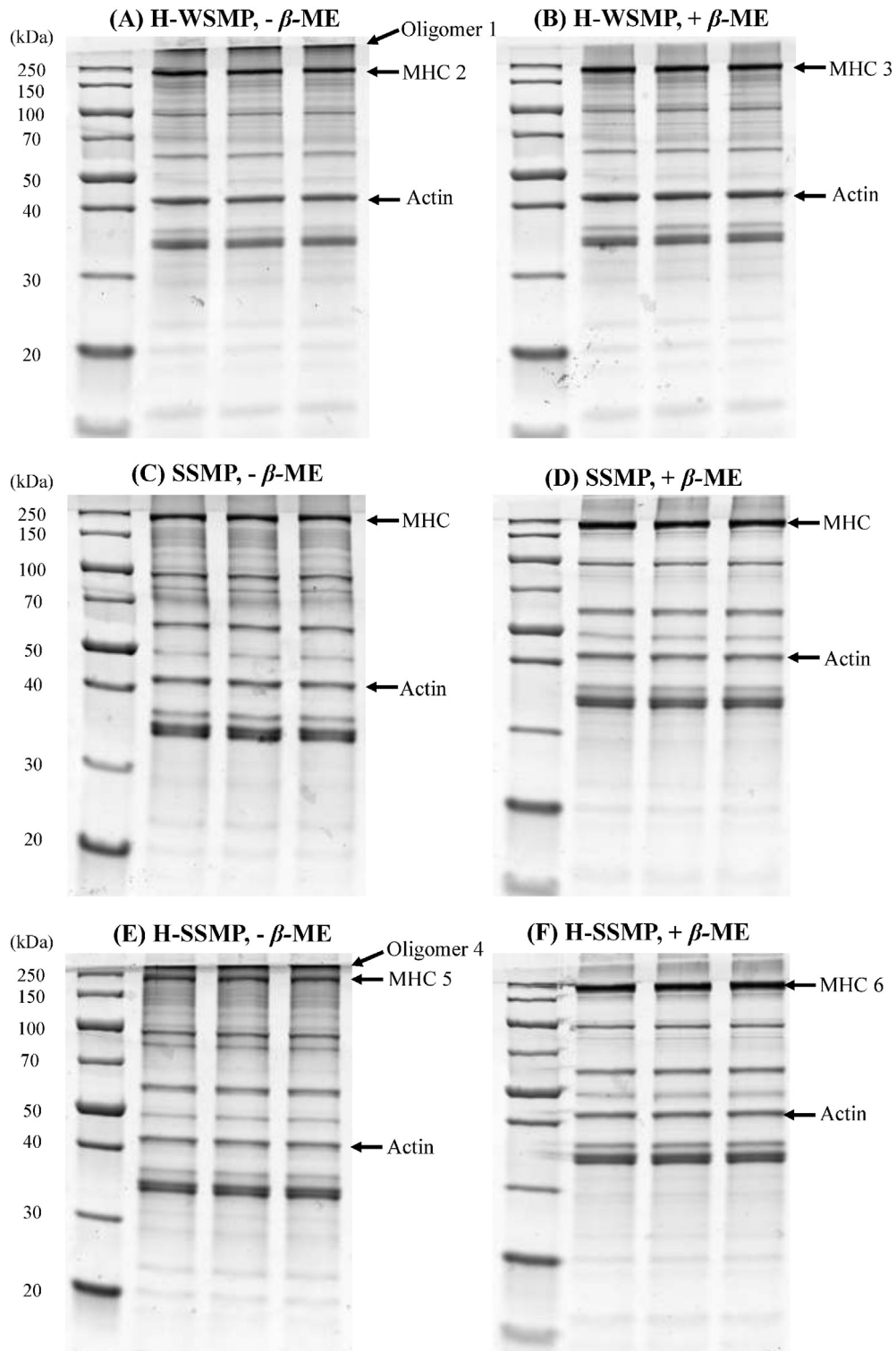


Fig. 1. Representative SDS-PAGE patterns of H-WSMP (A, B), SSMP (C, D) and H-SSMP (E, F). Samples were prepared in the absence of β -ME (A, C, E) or presence of β -ME (B, D, F). MHC: myosin heavy chain. The gel sections from the preparative lanes (oligomer 1, 4, MHC 2, 3, 5, 6) were sliced for LC-ESI-MS/MS analysis.

HPH treatment at 100 MPa. The increase in surface SH groups and hydrophobicity indicated the unfolding of MP structures induced by HPH. It has been reported that the intense mechanical forces occurring during HPH (high pressure plus shearing, turbulence and cavitation effects) can cause structural changes and denaturation of proteins (Keerati-u-rai & Corredig, 2009). Initially, high hydrostatic pressure allows water to penetrate the interior of the protein and modify protein conformation by affecting hydrogen and hydrophobic interactions, thus

disrupting the tertiary structures of MPs (Chen et al., 2014; Zhang, Yang, Tang, Chen, & You, 2015). When the MP suspension is forced through the homogenization valve at high speed, the strong shear stress, turbulence and cavitation phenomena, the predominant mechanisms of homogenization, give rise to dissociation, aggregation and/or rearrangement of colloidal particles and proteins (Liu & Kuo, 2016), resulting in the denaturation and unfolding of MPs. The unfolding of protein molecules may lead to exposure of SH and hydrophobic groups from

Table 1

Identified proteins and relative abundance from gel sections of the preparative lanes slices (oligomer 1, 4, MHC 2, 3, 5, 6 in Fig. 1) based on LC-ESI-MS/MS sequencing and analysis.

Band	Sequence header ^a	Protein mass (D) ^b	Relative abundance
(A) Oligomer 1	>sp P13538 MYSS_CHICK myosin heavy chain, skeletal muscle, adult OS = <i>Gallus gallus</i> PE = 1 SV = 4	223,974.73	60.4%
(A) MHC 2	>sp P13538 MYSS_CHICK myosin heavy chain, skeletal muscle, adult OS = <i>Gallus gallus</i> PE = 1 SV = 4	223,974.73	70.3%
(B) MHC 3	>sp P13538 MYSS_CHICK myosin heavy chain, skeletal muscle, adult OS = <i>Gallus gallus</i> PE = 1 SV = 4	223,974.73	97.0%
(E) Oligomer 4	>sp P13538 MYSS_CHICK myosin heavy chain, skeletal muscle, adult OS = <i>Gallus gallus</i> PE = 1 SV = 4	223,974.73	82.4%
(E) MHC 5	>sp P13538 MYSS_CHICK myosin heavy chain, skeletal muscle, adult OS = <i>Gallus gallus</i> PE = 1 SV = 4	223,974.73	84.8%
(F) MHC 6	>sp P13538 MYSS_CHICK myosin heavy chain, skeletal muscle, adult OS = <i>Gallus gallus</i> PE = 1 SV = 4	223,974.73	97.4%

^a The header of an identified protein present in NR database. It is limited to 300 characters.^b The calculated molecular weight of each identified protein based on its amino acid sequence present in the current NR database.

the interior of the native protein, which contributed to the increase of SH groups and surface hydrophobicity as observed in Fig. 2. It is noted that the greatest increase in SH groups and surface hydrophobicity occurred in H-SSMP and not that of H-WSMP (Fig. 2). This difference may be explained by greater access of HPH forces to the MP molecule at high ionic strength. At 0.6 M NaCl, the majority of MPs, e.g., myosin, was present as monomers, which were demonstrated to be more sensitive toward modification by HPH in comparison to the MPs in water where the majority of MPs were present as intact myofibril structures. It can be concluded that HPH caused the unfolding of MPs and increased the surface SH and hydrophobic groups.

MPs, especially myosin, are abundant in SH and hydrophobic residues, and are susceptible to chemical and physical modification (Li et al., 2012). It can be clearly seen that many buried SH groups

are exposed in H-WSMP via the denaturing process, either chemically and/or physically during HPH (Fig. 2). Myosin can form intermolecular disulfide linkages between SH groups that are exposed upon HPH treating as discussed in Fig. 1. It appears that the formation of myosin disulfide linkages occurred simultaneously with protein unfolding. In addition, the increase in surface SH content and hydrophobicity indicates an exposure of cysteine and hydrophobic amino acid residues that unfold on a protein surface. It is known that cysteine and all hydrophobic amino acid residues (e.g., tyrosine and phenylalanine) are negative in net charge at the experimental pH 7.0. Exposing the SH group and hydrophobic core would allow those initially buried negatively charged residues to be transferred to the protein surface, thereby increasing the surface negative charge of H-WSMP as we have previously reported (Chen et al., 2016a). Since NaCl at concentrations from 0.3 to 1.0 M induces a salting-in effect of MPs, it is thought that Cl⁻ ions bind to the filaments and increase the electrostatic repulsive forces between the filaments, allowing the filament lattice to expand and be solubilized in 0.6 M NaCl media (Offer & Trinick, 1983). Thus, we surmised that the increased negative charged residues induced by HPH might play the same role, thus rendering the solubilization of MPs in water.

3.3. Secondary structure of H-WSMP, SSMP and H-SSMP

The CD spectrum of native MPs in 0.6 M NaCl solution (SSMP) exhibited two negative bands near 208 and 222 nm (Fig. 3A), implying that the predominant form present was myosin tail, based on our knowledge of it having a supercoiled α -helix structure (Cao & Xiong, 2015; Li & Xiong, 2015). The CD pattern changed when MPs was subjected to HPH, where the distinct helical pattern underwent significant negative attenuation in the band regions of 208 and 222 nm (Fig. 3A), denoting significant disruptions of myosin helical structure (Cao & Xiong, 2015). The calculated α -helix content of SSMP (62%) was higher than the 58% reported by Chapleau, Mangavel, Compoint, and de Lamballerie-Anton (2004) which may be due to different meat sources and the extraction procedures employed. Compared to the native myosin in 0.6 M NaCl (SSMP), the α -helix content of H-WSMP significantly decreased ($P < 0.05$) from 62% to 57% (Fig. 3B). Because of the higher degree of MP denaturation in 0.6 M NaCl during HPH process, a further marked loss ($P < 0.05$) of α -helix content (decreased to around 52%) was observed for H-SSMP (Fig. 3B). These findings indicated that the conformational changes under HPH promoted loss of helicity of MPs in H-WSMP.

Progress in IR spectroscopic instrumentation has generated high expectations for the use of ATR-FTIR to study the secondary structural changes in proteins (Kong & Yu, 2007). Among the many benefits of FT-IR is its capacity to study protein structure in a large number of environments, including high protein concentrations and high salt media. Thus the secondary structure of MPs was also investigated with ATR-FTIR to elucidate the impact of HPH on modifying the MP structure in water and 0.6 M NaCl solution. The amide region (1700–1600 cm⁻¹) assigned to C=O stretching vibration is a sensitive indicator for the quantitative and qualitative determination of the secondary structure of proteins (Cando, Herranz, Borderias, & Moreno,

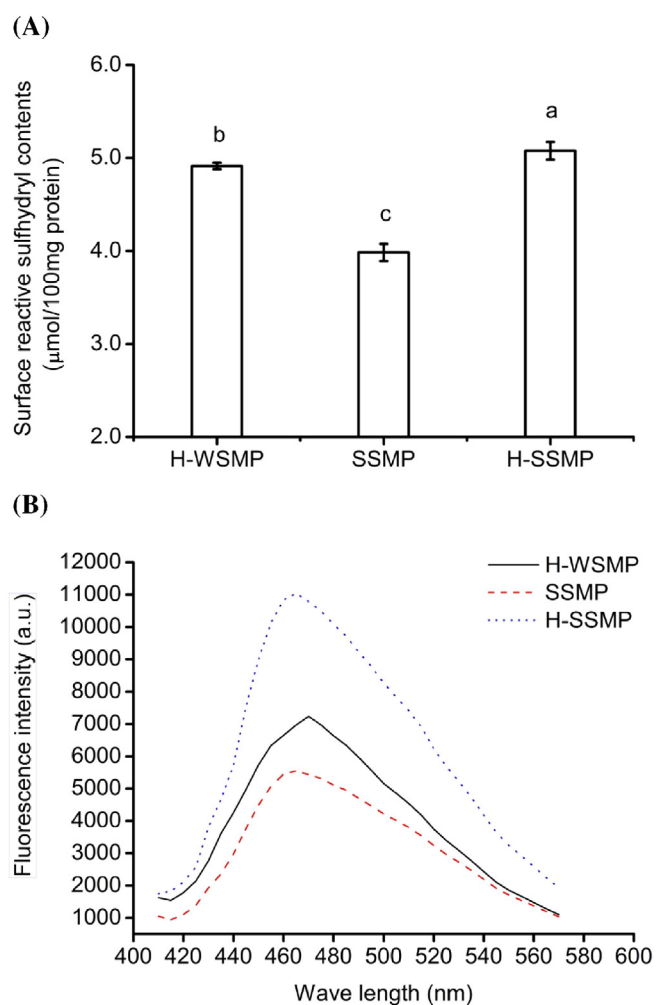
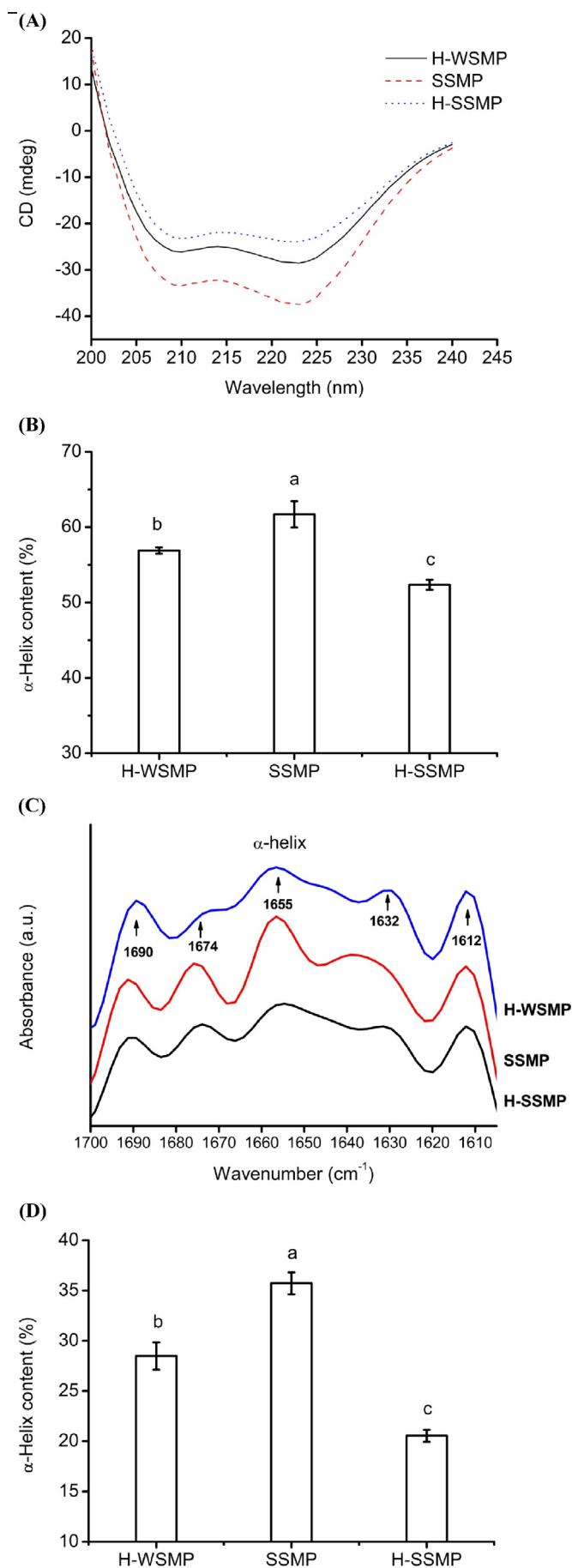


Fig. 2. Reactive sulfhydryl groups (A) and surface hydrophobicity (B) of H-WSMP, SSMP and H-SSMP. Values are means \pm SD ($n = 4$), a–c in (A) indicate significant differences ($P < 0.05$) between the preparations.



2015; Li & Xiong, 2015). The amide region showed five bands at wavenumbers: 1612, 1632, 1655, 1674 and 1690 cm^{-1} (Fig. 3C). The bands at 1610–1628 cm^{-1} , 1630–1640 cm^{-1} and 1690 cm^{-1} are related to aggregated β -sheet components and antiparallel β -sheet structures (Li & Xiong, 2015). The band near 1675 cm^{-1} is thought to originate from the structure of β -turn (Kong & Yu, 2007). The band near 1655 cm^{-1} can generally be assigned to an α -helical structure (Lee et al., 2007). As shown in Fig. 3C, SSMP showed a sharp peak at 1655 cm^{-1} , which is associated with α -helical structure of myosin in MPs (Li & Xiong, 2015). Upon HPH treatment, the intensity of band at 1655 cm^{-1} in both H-WSMP and H-SSMP decreased and the peak became wider (Fig. 3C). These modifications may be indicative of a decreased content of α -helical structure where the MPs were treated with HPH. With a view to providing more accurate information about the changes in the protein secondary structure, a quantitative estimation of α -helical structure was made as shown in Fig. 3D. The content of calculated α -helix in SSMP was 36%, which was slightly lower than the 62% obtained from the CD method. This difference was not unexpected given different principles of the methods and the protein concentrations required. Also, it is consistent with the ATR-FTIR result (35%) reported by Li and Xiong (2015). Upon HPH, significant losses ($P < 0.05$) were observed in the α -helix contents of both H-WSMP and H-SSMP (Fig. 3D). Again, the loss of α -helix resulting from HPH in H-SSMP (to 20%) was more extensive ($P < 0.05$) than that in H-WSMP (to 28%) (Fig. 3D). These results indicate partial unfolding of the proteins after HPH treatment.

Whether measured by CD or by ATR-FTIR, there was a general loss in α -helix contents of the proteins induced by HPH. This is consistent with the findings of Liu et al. (2010) who found a loss in the α -helix content in trypsin following HPH (80–120 MPa) induced by protein unfolding. Compared with the well-folded structure of the globular head (S1), the helical coiled-coil myosin tail (rod) is an elongated structure in which its amino acid side chain residue groups are more exposed and accessible to HPH. The 100% helical rod component in myosin has been found to represent the majority of the secondary structure spectra of MPs (Cao & Xiong, 2015). The α -helix structure of myosin is mainly stabilized by hydrogen bonds between the carbonyl oxygen ($-\text{CO}$) and amino hydrogen ($\text{NH}-$) of the polypeptide chain (Cao & Xiong, 2015; Liu, Zhao, Xiong, Xie, & Qin, 2008), HPH may have disturbed these hydrogen bonds, hence affecting its structure. In addition, the coiled-coil rod of myosin has a characteristic regular 7-residue pattern, where the hydrophobic residues are concentrated inside at alternate intervals along the length of the chain which tightly pack and stabilize the helix (Kristinsson & Hultin, 2003). HPH can cause unfolding of myosin and exposure of hydrophobic residues (Fig. 2B), thus resulting in the loss of α -helix in H-WSMP. Of all the myofibrillar components, myosin was the most affected protein, which was confirmed by SDS-PAGE as afore described. Loss of α -helix structure in the myosin rod region might cause a change in the interaction between the molecules, thus disrupting the filament assembly process, leading to enhanced solubility in water (Chen et al., 2016b).

3.4. Solubility and filament forming ability in low ionic strength solution

Native myosin (major protein in MPs) assembles and forms a filamentous polymer under low ionic strength conditions in vitro, which make it relatively insoluble in water or in dilute salt solutions (Chen et al., 2016b; Takai et al., 2013). To determine how the conformational changes of MPs induced by HPH influenced the myosin filament forming ability thereby solubility in water, the solubility and particle

Fig. 3. CD spectra (A) and deconvoluted spectra of amide I region of the ATR-FTIR spectra (C) of H-WSMP, SSMP and H-SSMP. The calculated α -helix structure contents from (A) and (C) were shown in (B) and (D), respectively. Values are means \pm SD ($n = 3$), a–c in (A2 and B2) indicate significant differences ($P < 0.05$) between the preparations.

size of each preparation H-WSMP, SSMP and H-SSMP when dialyzed in 1 mM NaCl were investigated.

Before dialysis, the MPs in H-WSMP, SSMP and H-SSMP were largely monomeric (Chen et al., 2016a; Takai et al., 2013) and it was expected that they would each display high solubility with a relative small average particle size of about 200 nm (Fig. 4A). Each MP solution (H-WSMP, SSMP and H-SSMP) displayed a clear, transparent state (Fig. 4B). After dialysis into 1 mM NaCl, where the ionic strength had decreased to 0.001, the native myosin in SSMP was able to polymerize to form filaments through rod-rod electrostatic interaction (Nakasawa et al., 2005; Sohn et al., 1997). Under these conditions the average particle size of D-SSMP was significantly ($P < 0.05$) increased to 2209 nm (Fig. 4A) where more than 80% of the native myosin molecules displayed an assembled filament state as observed by electron microscopy (Hayakawa et al., 2010; Sinard, Stafford, & Pollard, 1989). Due to the filament species scattering and the large particle size (micron range), the D-SSMP became opaque and insoluble in low ionic strength solutions (Fig. 4). This finding is consistent with literature reports, highlighting the insolubility of MPs in water in the absence of unique processing procedures (Chen et al., 2016a). Compared to the D-SSMP, both H-D-WSMP and H-D-SSMP exhibited relatively small particle size species (about 400 nm in the submicron range as shown in Fig. 4A), suggesting that the filament assembling process in H-WSMP and H-SSMP could not reach that achieved by SSMP during dialysis. This was also confirmed by photographic observation where a more transparent state was possessed by D-H-WSMP and D-H-SSMP than that of D-SSMP (Fig. 4B). Of particular interest is that a high solubility of 50% was still maintained in D-H-WSMP and D-H-SSMP, which was completely different to that of D-SSMP (Fig. 4A). It seems that the myosin filament forming ability was impaired in D-H-WSMP and D-H-SSMP. Therefore, we proposed that HPH might affect the myosin monomer-filament transition, thereby rendering higher solubility of MPs in water.

Some studies have demonstrated that conformation changes of myosin can influence the filament assembling process. A phenomenon has been reported that the lengthening of the LMM region of the myosin rod and the increase periodicity of LMM para-crystals induced by L-His led to the loss of chicken breast myosin filament forming ability (Hayakawa et al., 2009, 2010). The ability of L-His and L-lysine to induce the depolymerisation of pork myosin filament was thought to be caused by the loss of α -helical structures and the exposure of hydrophobic groups and masked SH groups to the surface (Guo et al., 2015). Thus, it is believed that the transformation of the myosin conformation after HPH treatment, as we discussed above, can inhibit filament assembly, resulting in high solubility of MPs in low ionic strength solutions.

On the basis of our results and previous studies, a model that explains the solubilization of MPs at low ionic solution (1 mM NaCl, pH 7.0) by HPH is proposed in Fig. 5. Myosin is the focal point in this mechanism because it is the predominant protein in MPs responsible for the overall solubility and it is the general target for modification by HPH. As depicted in Fig. 5, myosin mainly consists of two globular head regions and a rod-like tail portion consisting of a coiled-coil α -helix (Harrington & Rodgers, 1984). Myosin filaments disaggregate into myosin monomers in high ionic strength buffers (>0.3 M) and monomeric forms can subsequently re-aggregate back into filaments when the ionic strength is lowered (<0.3 M), thus determining the solubility under various conditions (Bandman et al., 1997; Sinard et al., 1989). The myosin rod is responsible for the self-association and formation of the filament in low ionic strength media. It has been shown that myosin can associate only through the C-terminal two-thirds of the myosin rod by electrostatic attractions between charged clusters in periodic distributions of the myosin-rod amino acid sequences (Nakasawa et al., 2005; Sohn et al., 1997). It is because of the formation of filamentous myosin that gives rise to the low solubility of MPs in aqueous solutions at low ionic strength (Fig. 4). However, HPH can cause unfolding of myosin, resulting in loss of α -helical structure

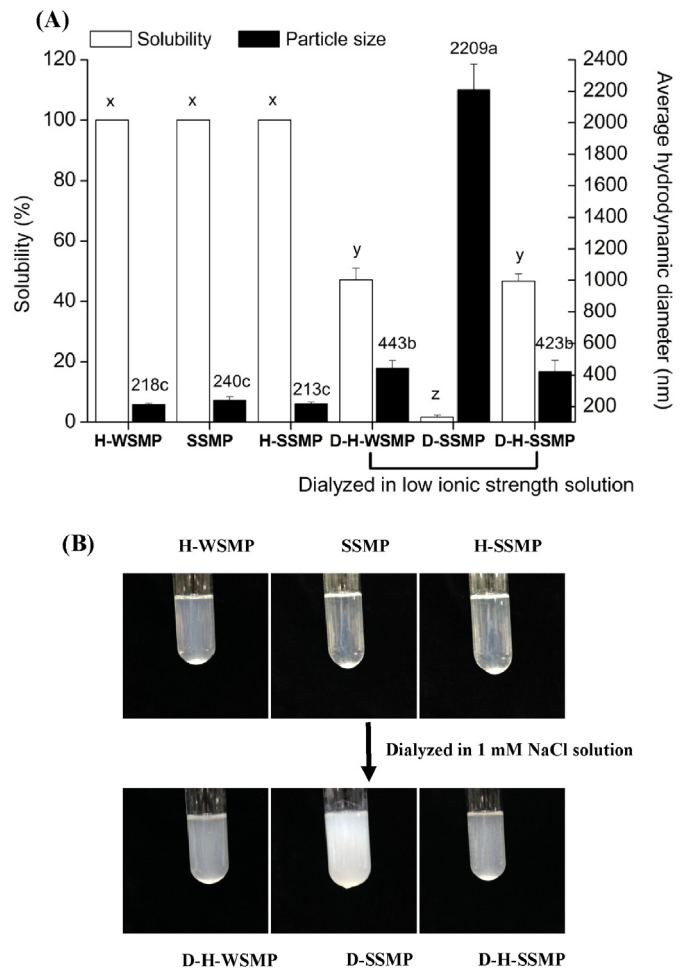


Fig. 4. (A) The solubility and particle size (average hydrodynamic diameter monitored by DLS at 25 °C) and (B) photographic representations of H-WSMP, SSMP, H-SSMP and the corresponding dialyzed samples (D-H-WSMP, D-SSMP and D-H-SSMP) in low ionic strength solution (1 mM KCl, pH 7.0). Values are means \pm SD ($n = 4$), x–z for solubility and a–c for particle size in (A) indicate significant differences ($P < 0.05$) between the preparations.

(Fig. 3) and exposure of buried hydrophobic and SH groups to the myosin surface (Fig. 2). This might induce changes in electrostatic forces between molecules, e.g., strengthen the inter-molecular electrostatic repulsion by exposure of negatively charged sites to the protein surface as discussed in Fig. 2. This would likely contribute to the weakening of the myosin filament-forming ability, which ultimately would increase the solubility of MPs in low ionic strength solutions (Fig. 4). In addition, HPH can form soluble myosin oligomer through S-S bonding, presumably in the rod (as discussed in Fig. 1). The covalent association of myosin rod may have imposed a steric hindrance, giving rise to increased protein solubility by inhibiting the filament formation of the rod region.

4. Conclusions

HPH caused significant uncoiling of the helical structure of myosin in MPs and subsequent protein unfolding and cross-linking: exposure of hydrophobic and SH groups and the formation of soluble myosin oligomers through disulfide bonds. As a result of these conformational changes, filament forming ability of myosin rod was impaired, and the MPs became soluble in water or low ionic strength solutions. Understanding the mechanism for the solubilization of MPs in water by HPH would advance the science of myofibrillar protein solubility and extend

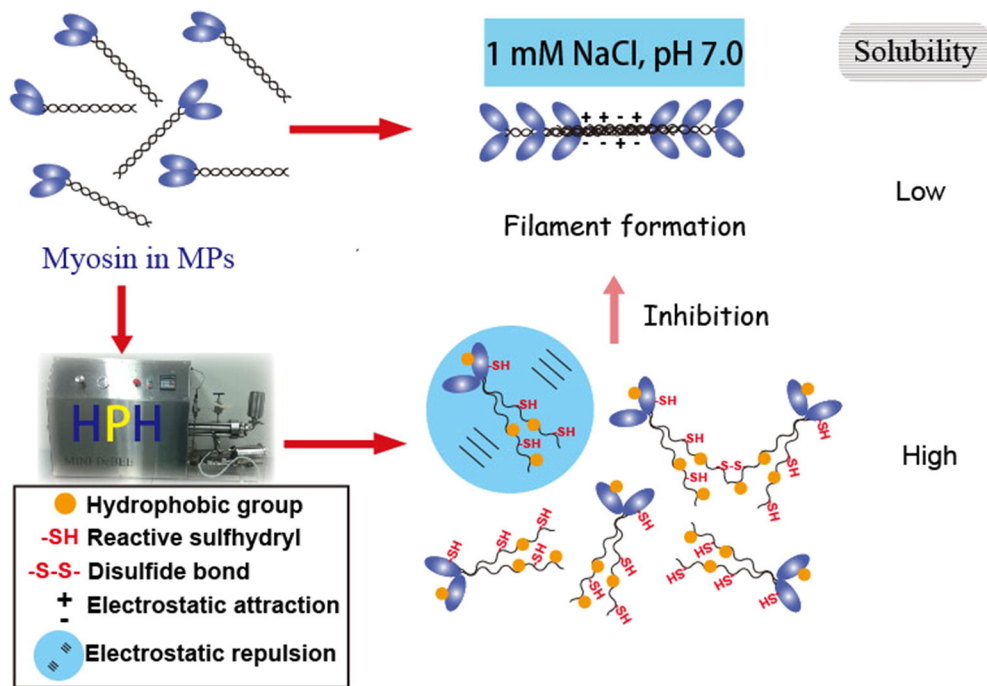


Fig. 5. Proposed mechanism of the solubilization of chicken breast MPs in water by HPH. See text for details.

the application area of HPH technology for development of new meat-based products in the food industry.

Acknowledgments

We gratefully acknowledge Dr. Ron Tume from CSIRO, Food and Nutrition Flagship, Brisbane, Australia for his valuable advice and for assistance with English language. This work was financially supported by the National Natural Science Foundation of China (No. 31471601), the China Agricultural Research System (Beijing, China, CARS-42) and a project funded by the Research and Innovation Project for Graduates of Jiangsu Province (No. KYLX15_0589).

References

- Bandman, E., Arrizubieta, M. J., Wick, M., Hattori, A., Tablin, F., Zhang, S., & Zhang, Q. (1997). Functional analysis of the chicken sarcomeric myosin rod: Regulation of dimerization, solubility, and fibrillogenesis. *Cell Structure and Function*, 22(1), 131–137.
- Cando, D., Herranz, B., Borderias, A. J., & Moreno, H. M. (2015). Effect of high pressure on reduced sodium chloride surimi gels. *Food Hydrocolloids*, 51, 176–187.
- Cao, Y., & Xiong, Y. L. (2015). Chlorogenic acid-mediated gel formation of oxidatively stressed myofibrillar protein. *Food Chemistry*, 180, 235–243.
- Cao, Y., Xia, T., Zhou, G., & Xu, X. (2012). The mechanism of high pressure-induced gels of rabbit myosin. *Innovative Food Science & Emerging Technologies*, 16, 41–46.
- Chapleau, N., Mangavel, C., Compoin, J. P., & de Lamballerie-Anton, M. (2004). Effect of high-pressure processing on myofibrillar protein structure. *Journal of the Science of Food and Agriculture*, 84(1), 66–74.
- Chen, X., Xu, X. L., & Zhou, G. H. (2016a). Potential of high pressure homogenization to solubilize chicken breast myofibrillar proteins in water. *Innovative Food Science & Emerging Technologies*, 33, 170–179.
- Chen, X., Zou, Y. F., Han, M. Y., Pan, L. H., Xing, T., Xu, X. L., & Zhou, G. H. (2016b). Solubilisation of myosin in a solution of low ionic strength L-histidine: Significance of the imidazole ring. *Food Chemistry*, 196, 42–49.
- Chen, X., Chen, C. G., Zhou, Y. Z., Li, P. J., Ma, F., Nishiumi, T., & Suzuki, A. (2014). Effects of high pressure processing on the thermal gelling properties of chicken breast myosin containing κ-carrageenan. *Food Hydrocolloids*, 40, 262–272.
- Griffin, N. M., Yu, J., Long, F., Oh, P., Shore, S., Li, Y., ... Schnitzer, J. E. (2010). Label-free, normalized quantification of complex mass spectrometry data for proteomic analysis. *Nature Biotechnology*, 28(1), 83–89.
- Guo, X. Y., Peng, Z. Q., Zhang, Y. W., Liu, B., & Cui, Y. Q. (2015). The solubility and conformational characteristics of porcine myosin as affected by the presence of L-lysine and L-histidine. *Food Chemistry*, 170, 212–217.
- Harrington, W. F., & Rodgers, M. E. (1984). Myosin. *Annual Review of Biochemistry*, 53(1), 35–73.
- Hayakawa, T., Ito, T., Wakamatsu, J., Nishimura, T., & Hattori, A. (2009). Myosin is solubilized in a neutral and low ionic strength solution containing L-histidine. *Meat Science*, 82(2), 151–154.
- Hayakawa, T., Ito, T., Wakamatsu, J., Nishimura, T., & Hattori, A. (2010). Myosin filament depolymerizes in a low ionic strength solution containing L-histidine. *Meat Science*, 84(4), 742–746.
- Ito, Y., Tatsumi, R., Wakamatsu, J. I., Nishimura, T., & Hattori, A. (2003). The solubilization of myofibrillar proteins of vertebrate skeletal muscle in water. *Animal Science Journal*, 74(5), 417–425.
- Katayama, S., & Saeki, H. (2007). Water solubilization of glycated carp and scallop myosin rods, and their soluble state under physiological conditions. *Fisheries Science*, 73(2), 446–452.
- Katayama, S., Haga, Y., & Saeki, H. (2004). Loss of filament-forming ability of myosin by non-enzymatic glycosylation and its molecular mechanism. *FEBS Letters*, 575(1), 9–13.
- Katayama, S., Shima, J., & Saeki, H. (2002). Solubility improvement of shellfish muscle proteins by reaction with glucose and its soluble state in low-ionic-strength medium. *Journal of Agricultural and Food Chemistry*, 50(15), 4327–4332.
- Keerati-u-rai, M., & Corredig, M. (2009). Effect of dynamic high pressure homogenization on the aggregation state of soy protein. *Journal of Agricultural and Food Chemistry*, 57(9), 3556–3562.
- Kong, J., & Yu, S. (2007). Fourier transform infrared spectroscopic analysis of protein secondary structures. *Acta Biochimica et Biophysica Sinica*, 39(8), 549–559.
- Kristinsson, H. G., & Hultin, H. O. (2003). Changes in conformation and subunit assembly of cod myosin at low and high pH and after subsequent refolding. *Journal of Agricultural and Food Chemistry*, 51(24), 7187–7196.
- Lee, S. H., Lefèvre, T., Subirade, M., & Paquin, P. (2007). Changes and roles of secondary structures of whey protein for the formation of protein membrane at soy oil/water interface under high-pressure homogenization. *Journal of Agricultural and Food Chemistry*, 55(26), 10924–10931.
- Li, C., & Xiong, Y. L. (2015). Disruption of secondary structure by oxidative stress alters the cross-linking pattern of myosin by microbial transglutaminase. *Meat Science*, 108, 97–105.
- Li, C., Xiong, Y. L., & Chen, J. (2012). Oxidation-induced unfolding facilitates myosin cross-linking in myofibrillar protein by microbial transglutaminase. *Journal of Agricultural and Food Chemistry*, 60(32), 8020–8027.
- Liu, H. H., & Kuo, M. I. (2016). Ultra high pressure homogenization effect on the proteins in soy flour. *Food Hydrocolloids*, 52, 741–748.
- Liu, W., Zhang, Z. Q., Liu, C. M., Xie, M. Y., Tu, Z. C., Liu, J. H., & Liang, R. H. (2010). The effect of dynamic high-pressure microfluidization on the activity, stability and conformation of trypsin. *Food Chemistry*, 123(3), 616–621.
- Liu, R., Zhao, S. M., Xiong, S. B., Xie, B. J., & Qin, L. H. (2008). Role of secondary structures in the gelation of porcine myosin at different pH values. *Meat Science*, 80(3), 632–639.
- Nakasawa, T., Takahashi, M., Matsuzawa, F., Aikawa, S., Togashi, Y., Saitoh, T., ... Yazawa, M. (2005). Critical regions for assembly of vertebrate nonmuscle myosin II. *Biochemistry*, 44(1), 174–183.
- Nieuwenhuizen, W. F., Weenen, H., Rigby, P., & Hetherington, M. M. (2010). Older adults and patients in need of nutritional support: Review of current treatment options and factors influencing nutritional intake. *Clinical Nutrition*, 29(2), 160–169.

- Offer, G., & Trinick, J. (1983). On the mechanism of water holding in meat: The swelling and shrinking of myofibrils. *Meat Science*, 8(4), 245–281.
- Ooizumi, T., & Xiong, Y. L. (2006). Identification of cross-linking site(s) of myosin heavy chains in oxidatively stressed chicken myofibrils. *Journal of Food Science*, 71(3), C196–C199.
- Pereda, J., Ferragut, V., Quevedo, J., Guamis, B., & Trujillo, A. (2007). Effects of ultra-high pressure homogenization on microbial and physicochemical shelf life of milk. *Journal of Dairy Science*, 90(3), 1081–1093.
- Saeki, H., & Inoue, K. (1997). Improved solubility of carp myofibrillar proteins in low ionic strength medium by glycosylation. *Journal of Agricultural and Food Chemistry*, 45(9), 3419–3422.
- Shimada, M., Takai, E., Ejima, D., Arakawa, T., & Shiraki, K. (2015). Heat-induced formation of myosin oligomer-soluble filament complex in high-salt solution. *International Journal of Biological Macromolecules*, 73, 17–22.
- Sinard, J. H., Stafford, W. F., & Pollard, T. D. (1989). The mechanism of assembly of acanthamoeba myosin-II minifilaments: Minifilaments assemble by three successive dimerization steps. *The Journal of Cell Biology*, 109(4), 1537–1547.
- Sohn, R. L., Vikstrom, K. L., Strauss, M., Cohen, C., Szent-Gyorgyi, A. G., & Leinwand, L. A. (1997). A 29 residue region of the sarcomeric myosin rod is necessary for filament formation. *Journal of Molecular Biology*, 266(2), 317–330.
- Takai, E., Yoshizawa, S., Ejima, D., Arakawa, T., & Shiraki, K. (2013). Synergistic solubilization of porcine myosin in physiological salt solution by arginine. *International Journal of Biological Macromolecules*, 62, 647–651.
- Tokifuji, A., Matsushima, Y., Hachisuka, K., & Yoshioka, K. (2013). Texture, sensory and swallowing characteristics of high-pressure-heat-treated pork meat gel as a dysphagia diet. *Meat Science*, 93(4), 843–848.
- Xiong, Y. L., Park, D., & Ooizumi, T. (2008). Variation in the cross-linking pattern of porcine myofibrillar protein exposed to three oxidative environments. *Journal of Agricultural and Food Chemistry*, 57(1), 153–159.
- Yuan, Y., Gao, Y., Zhao, J., & Mao, L. (2008). Characterization and stability evaluation of β -carotene nanoemulsions prepared by high pressure homogenization under various emulsifying conditions. *Food Research International*, 41(1), 61–68.
- Zhang, Z., Yang, Y., Tang, X., Chen, Y., & You, Y. (2015). Chemical forces and water holding capacity study of heat-induced myofibrillar protein gel as affected by high pressure. *Food Chemistry*, 188, 111–118.